Anti-Stokes Laser Cooling in Bulk Erbium-Doped Materials

Joaquin Fernandez,[1,2,*] Angel J. Garcia-Adeva,[1] and Rolindes Balda[1,2]

[1]*Departamento de Fisica Aplicada I, E.T.S. Ingenieria de Bilbao, Alda. Urquijo s/n, 48013 Bilbao, Spain*

[2]*Unidad Fisica de Materiales CSIC-UPV/EHU and Donostia International Physics Center, Apartado 1072, 20080 San Sebastian, Spain*

(Received 5 May 2006; published 18 July 2006)

We report the first observation of anti-Stokes laser-induced cooling in the Er^{3+}:KPb_2Cl_5 crystal and in the Er^{3+}:CNBZn (CdF_2-$CdCl_2$-NaF-BaF_2-$BaCl_2$-ZnF_2) glass. The internal cooling efficiencies have been calculated by using photothermal deflection spectroscopy. Thermal scans acquired with an infrared thermal camera proved the bulk cooling capability of the studied samples. The implications of these results are discussed.

DOI: 10.1103/PhysRevLett.97.033001 PACS numbers: 32.80.Pj, 42.55.Rz, 44.40.+a, 78.55.−m

The basic principle that anti-Stokes fluorescence might be used to cool a material was first postulated by Pringsheim in 1929. Twenty years later, Kastler suggested [1] that rare-earth-doped crystals might provide a way to obtain solid-state cooling by anti-Stokes emission (CASE). A few years later, the invention of the laser promoted the first experimental attempt by Kushida and Geusic to demonstrate radiation cooling in a Nd^{3+}:YAG crystal [2]. However, it was not until 1995 that the first solid-state CASE was convincingly proven by Epstein and co-workers in an ytterbium-doped heavy-metal fluoride glass [3]. Since then, the efforts to develop other different materials doped with rare-earth (RE) ions were unsuccessful due to the inherent characteristics of the absorption and emission processes in RE ions. In most of the materials studied, the presence of nonradiative (NR) processes hindered the CASE performance. As a rule of thumb, a negligible impurity parasitic absorption and near-unity quantum efficiency of the anti-Stokes emission from the RE levels involved in the cooling process are required, so that NR transition probabilities by multiphonon emission or whatever other heat generating process remain as low as possible. These constraints could explain why most of the efforts to obtain CASE in condensed matter were performed on trivalent ytterbium-doped solids (glasses [4] and crystals [5,6]) having only one excited state manifold which is placed $\sim 10\,000\ cm^{-1}$ above the ground state. The only exception was the observation of CASE in a thulium-doped glass by using the transitions between the $^3H_6$ and $^3H_4$ manifolds to cool down the sample [7]. Therefore, it is easy to see that identifying new optically active ions and materials capable of producing CASE is still an open problem with very important implications from both the fundamental and practical points of view.

On the other hand, the recent finding of new low phonon materials (both glasses [8] and crystals [6]) as RE hosts which may significantly decrease the NR emissions from excited state levels have renewed the interest in investigating new RE anti-Stokes emission channels. In this work, we present the first experimental demonstration of anti-Stokes laser-induced cooling in two different erbium-doped matrices: a low phonon KPb_2Cl_5 crystal and a fluorochloride glass. In order to assess the presence of internal cooling in these systems, we employed the photothermal deflection technique, whereas the bulk cooling was detected by means of a calibrated thermal sensitive camera. The cooling was obtained by exciting the Er^{3+} ions at the low energy side of the $^4I_{9/2}$ manifold with a tunable Ti:sapphire laser. It is worthwhile to mention that this excited state where cooling can be induced is also involved in infrared to visible up-conversion processes [9]. However, these nonlinear processes occur in a slightly different spectral region, and, thus, they do not contribute to the observed cooling. Moreover, it is also noticeable that the laser-induced cooling can be easily reached at wavelengths and powers at which conventional laser diodes operate, which renders these systems very convenient for applications, such as compact solid-state optical cryocoolers.

Single crystals of nonhygroscopic Er^{3+}:KPb_2Cl_5 were grown in our laboratory by the Bridgman technique [10]. The rare-earth content was 0.5 mol % of $ErCl_3$. The fluorochloride CNBZn glass doped with 0.5 mol % of ErF_3 was synthesized at the Laboratoire de Verres et Ceramiques of the University of Rennes. The experimental setup and procedure for photothermal deflection measurements have been described elsewhere [8,11]. The beam of a tunable cw Ti:sapphire ring laser (Coherent 899), with a maximum output power of 2.5 W, was modulated at low frequency (1–10 Hz) by a mechanical chopper and focused into the middle of the sample with a diameter of $\sim 100\ \mu m$. The copropagating helium-neon probe laser beam ($\lambda = 632.8$ nm) was focused to $\sim 60\ \mu m$, coaligned with the pump beam, and its deflection detected by a quadrant position detector. The samples (of sizes $4.5 \times 6.5 \times 2.7$ and $10.7 \times 10.7 \times 2.2\ mm^3$ for the crystal and glass, respectively) were freely placed on a Teflon holder inside a low vacuum ($\sim 10^{-2}$ mbar) cryostat chamber at room temperature.

The cooling efficiencies of the Er^{3+}-doped materials were evaluated at room temperature by measuring the

quantum efficiency (QE) of the emission from the $^4I_{9/2}$ manifold in the heating and cooling regions by means of the photothermal deflection spectroscopy in a collinear configuration [8,11]. The evaluation of the QE has been carried out by considering a simplified two level system for each of the transitions involved. In the photothermal collinear configuration, the amplitude of the angular deviation of the probe beam is always proportional to the amount of heat the sample exchanges, whatever its optical or thermal properties are. The QE of the transition, η, can be obtained from the ratio of the photothermal deflection amplitude (PDS) to the sample absorption (Abs) obtained as a function of the excitation wavelength λ around the mean fluorescence wavelength λ_0

$$\frac{\mathrm{PDS}}{\mathrm{Abs}} = C\left(1 - \eta\frac{\lambda}{\lambda_0}\right), \tag{1}$$

where C is a proportionality constant that depends on the experimental conditions. The mean fluorescence wavelength, above which cooling is expected to occur, was calculated by taking into account the branching ratios for the emissions from level $^4I_{9/2}$. As expected, the calculated value is close to that found experimentally for the transition wavelength at which the cooling region begins.

Figure 1(a) shows the normalized PDS spectrum of the Er^{3+}:KPb_2Cl_5 crystal around the zero deflection signal (852.5 nm)—obtained at an input power of 1.5 W—together with the best least-squares fitting in both the heating and cooling regions. The resulting QE values are $0.999\,73 \pm 0.000\,08$ and $1.003\,45 \pm 0.000\,04$, respectively, and, therefore, the cooling efficiency estimated by using the QE measurements is $0.37 \pm 0.01\%$. As predicted by the theory [12], a sharp jump of 180° in the PDS phase measured by lock-in detection can be observed during the transition from the heating to the cooling region [see Fig. 1(b)]. Figure 1(c) shows the PDS amplitude waveforms registered in the oscilloscope at three different excitation wavelengths: 800 (heating region), 852.5 (mean fluorescence wavelength), and 870 nm (cooling region). As can be noticed, at 852.5 nm the signal is almost zero, whereas in the cooling region, at 870 nm, the waveform of the PDS signal shows an unmistakable phase reversal of 180° when compared with the one at 800 nm. Figure 2 shows the CASE results for the Er^{3+}:CNBZn glass (obtained at a pump power of 1.9 W) where the zero deflection signal occurs around 843 nm. The 180° change of the PDS phase is also clearly attained but with a little less sharpness than for the Er^{3+}:KPb_2Cl_5 crystal [see Fig. 2(b)]. The QE values corresponding to the heating and cooling regions are $0.997\,64 \pm 0.000\,05$ and $1.004\,46 \pm 0.000\,01$, respectively, and the estimated cooling efficiency is $0.682 \pm 0.006\%$. The PDS waveforms corresponding to the heating and cooling regions are shown in Fig. 2(c). It is worthy to notice that the cooling processes in both systems can be obtained at quite low power excitations. As an example, for

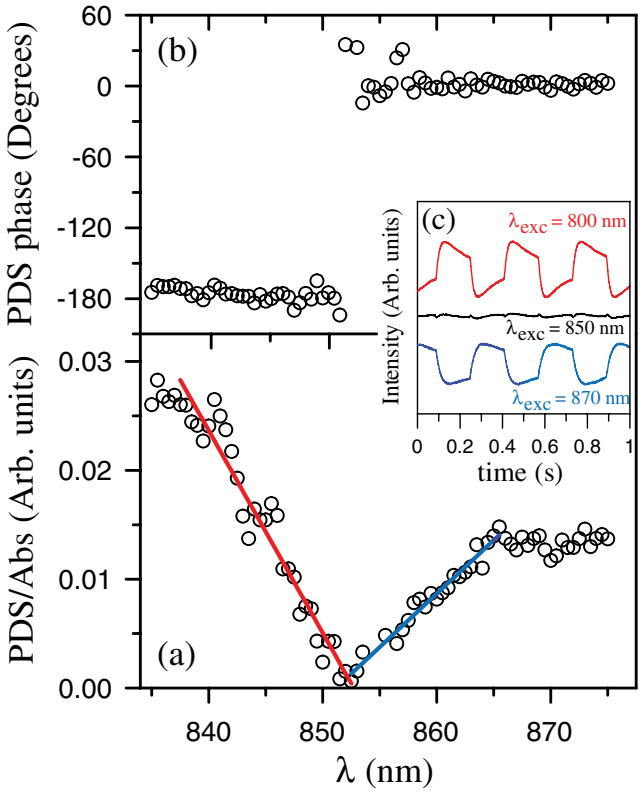

FIG. 1 (color). (a) Signal deflection amplitude normalized by the sample absorption as a function of pumping wavelength for the Er^{3+}:KPb_2Cl_5 crystal. (b) Phase of the photothermal deflection signal as a function of pumping wavelength. (c) Photothermal deflection signal waveforms in the heating (800 nm) and cooling (870 nm) regions and around the cooling threshold (850 nm).

the Er^{3+}:KPb_2Cl_5 crystal, CASE is still efficient at a pump power of only 500 mW.

The results described in the previous paragraphs clearly demonstrate that these systems are capable of internal laser cooling in a certain spectral range and even at small pumping powers. We also conducted measurements of the absolute temperature of the present materials as a function of time for several pumping powers between 0.25 and 1.9 W and wavelengths in both the heating and cooling regions described above in order to assess quantitatively their cooling potential. To perform these measurements, a Thermacam SC 2000 (FLIR Systems) infrared thermal camera was used. This camera operates between −40 and 500 °C object temperature with a precision of ±0.1 °C. The detector is an array of 320 × 240 microbolometers. The camera is connected to an acquisition card interface that is able to record thermal scans at a rate of 50 Hz. The absolute temperature was calibrated with a thermocouple located at the sample holder.

Thermal scans at a rate of 1 image per second were acquired for time intervals that depend on the particular data series. The camera was placed 12 cm apart from the

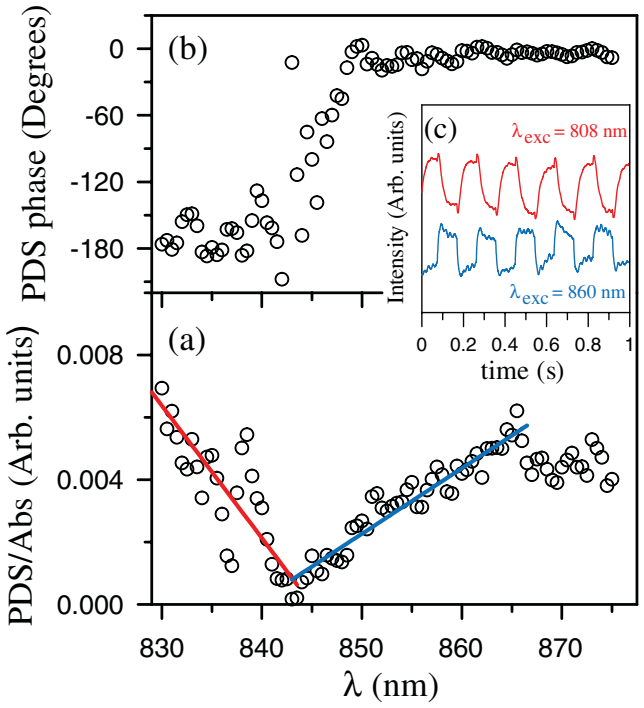

FIG. 2 (color). (a) Signal deflection amplitude normalized by the sample absorption as a function of pumping wavelength for the Er^{3+}:CNBZn glass. (b) Phase of the photothermal deflection signal as a function of pumping wavelength. (c) Photothermal deflection signal waveforms in the heating (808 nm) and cooling (860 nm) regions.

window cryostat so that a lens with a field of vision of 45° allows focusing the camera on the sample. Figures 3 and 4 show the runs performed at 870 and 860 nm for the Er^{3+}:KPb_2Cl_5 crystal and Er^{3+}:CNBZn glass samples, respectively, using the same pump geometry conditions as the ones described above. The laser power on the sample was fixed at 1.9 W in both cases. According to the PDS measurements reported above, these pumping wavelengths are well inside the cooling region for both materials. The insets in Figs. 3 and 4 depict some examples of the thermal scans obtained with the infrared camera. It is clear from those colormaps that the sample is cooling down as time goes by. However, it is difficult to extract any quantitative information about the amount the sample is cooling, as these changes are small compared with the absolute temperature of its surroundings. For this reason, in order to assess whether cooling is occurring in the bulk, we calculated the average temperature of the area enclosed in the green rectangles depicted in the upper insets in Figs. 3 and 4 and the corresponding results constitute the green curves in those figures. As it is easy to see, both samples cool down under laser irradiation. The Er^{3+}:KPb_2Cl_5 sample temperature drops by 0.7 ± 0.1 °C in 1500 s. To check that this temperature change was indeed due to laser cooling, the laser was turned off at that point. This can be easily identified as an upturn in the curve that represents the

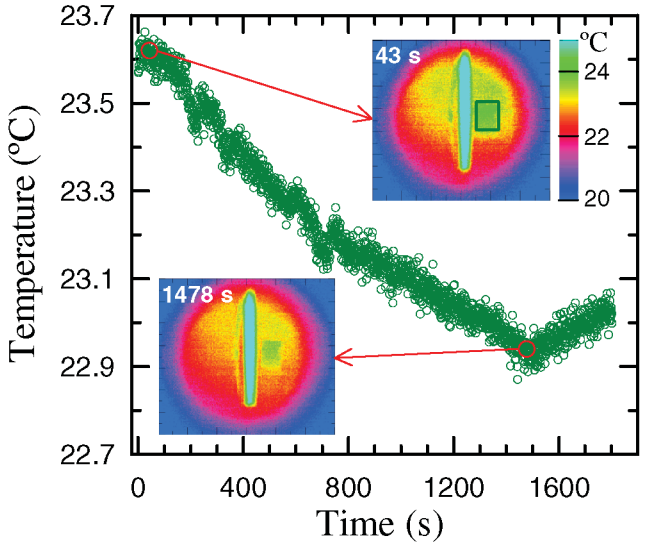

FIG. 3 (color). Time evolution of the average temperature of the Er^{3+}:KPb_2Cl_5 at 870 nm. The insets show colormaps of the temperature field of the whole system (sample plus cryostat) at two different times as measured with the thermal camera. The rectangle in the upper inset delimits the area used for calculating the average temperature of the sample.

evolution of the sample temperature, which means that this quantity starts to rise as soon as the laser irradiation is stopped. On the other hand, the temperature of the Er^{3+}:CNBZn glass sample starts to rise when laser irradiation starts. After ~150 s, this tendency is inverted and the sample starts to cool down. From that point on (and in approximately 1000 s), the average temperature of the

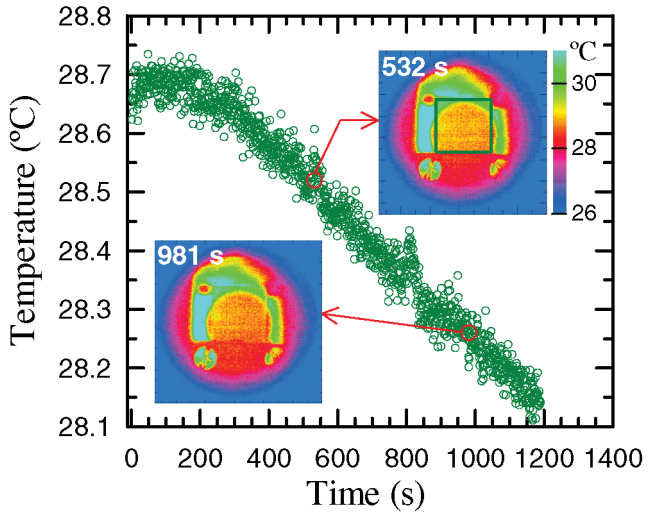

FIG. 4 (color). Time evolution of the average temperature of the Er^{3+}:CNBZn at 860 nm. The insets show colormaps of the temperature field of the whole system (sample plus cryostat) at two different times as measured with the thermal camera. The rectangle in the upper inset delimits the area used for calculating the average temperature of the sample.

sample drops by 0.5 ± 0.1 °C. Estimations of the expected bulk temperature change based on microscopic models proposed by Petrushkin, Samartev, and Adrianov [13] yield values of -5 and -10 °C for the crystalline and glass samples, respectively, under the experimental conditions described above. The discrepancy between the theoretical estimates and the present experimental results can be attributed to partial reabsorption of the anti-Stokes fluorescence, not taken into account in these models, or additional absorption processes of the pumping radiation involving excited states, which are known to be significant in these materials [9]. In any case, if one takes into account the minute concentrations of the optically active ions in the materials studied in this work and the geometry of the cooling experiment (single pass configuration), we think that the results described in this paragraph come to show that CASE in these materials is extremely efficient.

In conclusion, we have demonstrated cooling by anti-Stokes emission in two materials doped with Er optically active ions by using a combination of photothermal deflection measurements and time evolution of the average temperature of the sample acquired with an infrared camera. In particular, the photothermal deflection measurements clearly show internal cooling in the two samples analyzed. The cooling efficiencies are found to be about 0.4% and 0.7% for the crystal and glass samples, respectively. These figures are remarkable if one takes into account the fact that the concentration of the optically active ions in our materials is about 0.5% of Er^{3+} and that our experiments are performed in a single pass configuration. From a fundamental perspective, these results are quite important, as this ion comes to engross the small list of rare-earth ions that are amenable to cooling (Yb^{3+} and Tm^{3+} ions being the other two known so far). On the other hand, the measurements performed by using the infrared camera demonstrate that the Er^{3+} ions present in the materials are able to refrigerate these by 0.7 and 0.5 °C for the crystalline and glass samples, respectively. This result is extremely important from the applied point of view, as it paves the way to use this ion as an efficient anti-Stokes emitter for compact solid-state optical refrigerators. Moreover, it opens a wide field of applications related to the possibility to use CASE to offset the heat generated by the laser operation in Er^{3+}-based fiber lasers—the so-called radiation-balanced lasers [14]—that would allow one to use dual wavelength pumping to take advantage of the cooling processes occurring at a given wavelength. This technique could allow one to scale up the power of Er^{3+}-based fiber lasers. On the other hand, the use of Er^{3+}-doped nanoparticles for bioimaging or phototherapy could also take advantage of a dual wavelength pumping (at a nearby wavelength) in order to balance the thermal damage produced in a soft tissue by the infrared pumping wavelength at which the up-conversion process occurs.

This work was supported by the University of the Basque Country (Grant No. UPV13525/2001). A. J. G.-A. acknowledges financial support from the Spanish MEC under the ''Ramon y Cajal'' program. The authors thank Professor J. L. Adam for supplying the glass sample.

*Electronic address: wupferoj@bi.ehu.es

[1] A. Kastler, J. Phys. Radium **11**, 255 (1950).
[2] T. Kushida and J. E. Geusic, Phys. Rev. Lett. **21**, 1172 (1968).
[3] R. I. Epstein, M. I. Buchwald, B. C. Edwards, T. R. Gosnell, and C. E. Mungan, Nature (London) **377**, 500 (1995).
[4] C. W. Hoyt, M. P. Hasselbeck, M. Sheik-Bahae, R. I. Epstein, S. Greenfield, J. Thiede, J. Distel, and J. Valencia, J. Opt. Soc. Am. B **20**, 1066 (2003), and references therein; A. Rayner, N. R. Heckenberg, and H. Rubinsztein-Dunlop, J. Opt. Soc. Am. B **20**, 1037 (2003), and references therein.
[5] S. R. Bowman and C. E. Mungan, Appl. Phys. B **71**, 807 (2000); R. I. Epstein, J. J. Brown, B. C. Edwards, and A. Gibbs, Appl. Phys. Lett. **90**, 4815 (2001).
[6] A. Mendioroz, J. Fernandez, M. Voda, M. Al-Saleh, R. Balda, and A. J. Garcia-Adeva, Opt. Lett. **27**, 1525 (2002).
[7] C. W. Hoyt, M. Sheik-Bahae, R. I. Epstein, B. C. Edwards, and J. E. Anderson, Phys. Rev. Lett. **85**, 3600 (2000).
[8] J. Fernandez, A. Mendioroz, A. J. Garcia, R. Balda, and J. L. Adam, Phys. Rev. B **62**, 3213 (2000).
[9] R. Balda, A. J. Garcia-Adeva, M. Voda, and J. Fernandez, Phys. Rev. B **69**, 205203 (2004).
[10] M. Voda, M. Al-Saleh, G. Lobera, R. Balda, and J. Fernandez, Opt. Mater. (N.Y.) **26**, 359 (2004).
[11] J. Fernandez, A. Mendioroz, A. J. Garcia, R. Balda, and J. L. Adam, J. Alloys Compd. **323–324**, 239 (2001).
[12] W. B. Jackson, N. M. Amer, A. C. Boccara, and D. Fournier, Appl. Opt. **20**, 1333 (1981).
[13] S. V. Petrushkin and V. V. Samartsev, Theor. Math. Phys. (Engl. Transl.) **126**, 136 (2001); S. N. Adrianov and V. V. Samartsev, Laser Phys. **9**, 1021 (1999).
[14] S. R. Bowman, IEEE J. Quantum Electron. **35**, 115 (1999).